Beamforming and Jamming Optimization for IRS-Aided Secure NOMA Networks

Wei Wang, *Graduate Student Member, IEEE,* Xin Liu, *Senior Member, IEEE,* Jie Tang, *Senior Member, IEEE,* Nan Zhao, *Senior Member, IEEE,* Yunfei Chen, *Senior Member, IEEE,* Zhiguo Ding, *Fellow, IEEE,* and Xianbin Wang, *Fellow, IEEE*

***Abstract*—The integration of intelligent reflecting surface (IRS) and multiple access provides a promising solution to improved coverage and massive connections at low cost. However, securing IRS-aided networks remains a challenge since the potential eavesdropper also has access to an additional IRS reflection link, especially when the eavesdropping channel state information is unknown. In this paper, we propose an IRS-assisted non-orthogonal multiple access (NOMA) scheme to achieve secure communication via artificial jamming, where the multi-antenna base station sends the NOMA and jamming signals together to the legitimate users with the assistance of IRS, in the presence of a passive eavesdropper. The sum rate of legitimate users is maximized by optimizing the transmit beamforming, the jamming vector and the IRS reflecting vector, satisfying the quality of service requirement, the IRS reflecting constraint and the successive interference cancellation (SIC) decoding condition. In addition, the received jamming power is adapted at the highest level at all legitimate users for successful cancellation via SIC. To tackle this non-convex optimization problem, we first decompose it into two subproblems, and then each subproblem is converted into a convex one using successive convex approximation. An alternate optimization algorithm is proposed to solve them iteratively. Numerical results show that the secure transmission in the proposed IRS-NOMA scheme can be effectively guaranteed with the assistance of artificial jamming.**

***Index Terms*—Artificial jamming, beamforming optimization, intelligent reflecting surface, non-orthogonal multiple access, physical layer security.**

Manuscript received December 4, 2020; revised April 26, 2021 and August 9, 2021; accepted August 11, 2021. The work was supported by the National Key R&D Program of China under Grant 2020YFB1807002, the National Natural Science Foundation of China (NSFC) under Grant 61871065, and the open research fund of State Key Laboratory of Integrated Services Networks under Grant ISN22-22. Part of this work is presented in IEEE/CIC ICCC'21 [1]. The associate editor coordinating the review of this paper and approving it for publication was T. Q. Duong. *(Corresponding author: Nan Zhao.)*

W. Wang, X. Liu and N. Zhao are with the Key Laboratory of Intelligent Control and Optimization for Industrial Equipment of Ministry of Education, Dalian University of Technology, Dalian 116024, P. R. China, and also with the State Key Laboratory of Integrated Services Networks, Xidian University, Xi'an 710071, P. R. China (email: 21809066@mail.dlut.edu.cn, liuxinstar1984@dlut.edu.cn, zhaonan@dlut.edu.cn).

J. Tang is with the School of Electronic and Information Engineering, South China University of Technology, Guangzhou, China. (e-mail: eejtang@scut.edu.cn).

Y. Chen is with the School of Engineering, University of Warwick, Coventry CV4 7AL, U.K. (e-mail: Yunfei.Chen@warwick.ac.uk).

Z. Ding is with the School of Electrical and Electronic Engineering, The University of Manchester, Manchester, M13 9PL, U.K. (e-mail: zhiguo.ding@manchester.ac.uk).

X. Wang is with the Department of Electrical and Computer Engineering, Western University, London, ON N6A 5B9, Canada (e-mail: xianbin.wang@uwo.ca).

I. Introduction

Intelligent reflecting surface (IRS) is a promising technique to improve communication quality via reconfiguration of propagation environment [2]. As a two-dimensional surface consisting of a large number of passive reconfigurable reflecting units, IRS can be flexibly deployed on the facade of buildings. Compared with traditional relays, IRS consumes less power because it only reflects signals by using low-cost reflecting elements [3], [4]. On the other hand, due to its flexible reconfigurability of IRS, it can easily work in the full-duplex mode without involving interference [5]. Therefore, IRS has drawn tremendous attention from both academia and industry recently [6].

IRS has a great potential to enhance physical layer security (PLS) for wireless networks [7]–[11], as the reflected signal can be beamformed at legitimate receivers and suppressed at the eavesdropper by adjusting IRS reflecting elements. In [7], Chen *et al.* proposed a programmable secure wireless environment using this reconfiguration capability of IRS. Thus, there is no need to deploy extra relay or jammer to degrade the reception at the eavesdropper, which greatly reduces the transmission power. In [8], the achievable secrecy rate of an IRS-assisted system was maximized by Guan *et al.* via jointly optimizing the precoding with artificial noise and IRS beamforming. The exceptional performance of IRS in secure transmission has been utilized in both multi-input single-output (MISO) and multi-input multi-output (MIMO) systems [9], [10]. Furthermore, the secure communication of IRS-MISO systems was investigated in [11] by Yu *et al.*, taking into account the imperfect channel state information (CSI) of eavesdropping channels. However, all these works are based on the assumption that the full CSI or partial CSI of the eavesdropper is available in legitimate networks [7]–[11], which is challenging in practice since the eavesdropper is usually passive and does not actively exchange its CSI with the transmitter.

On the other hand, non-orthogonal multiple access (NOMA) is considered as an effective solution to enhancing spectrum efficiency and achieving massive connectivity in future wireless networks [12], [13]. Different from the conventional orthogonal multiple access (OMA), the power-domain NOMA allows the allocation of the resource block (i.e., frequence/code) to multiple users simultaneously [14]. At the transmitter, the signals for different users use different power levels according to the difference in channel gain, and then superimposed in

the power domain. At the receiver, successive interference cancellation (SIC) is utilized to eliminate the multiple-access interference and decode the desired information [15]. Due to its concurrent communications nature, NOMA systems are susceptible to different security and confidentiality related issues. To guarantee the secure transmission in NOMA networks, various PLS methods have been proposed, e.g., beamforming [16]–[18], cooperative relaying [19], [20], artificial jamming [21], [22], *etc*.

Nevertheless, it is worth noticing that NOMA can achieve better spectrum efficiency than OMA only when the channel gains of the users are considerably different. Since IRS can digitally adjust the phase shift of reflected signals, it has a great potential to enhance the channel difference and obtain the NOMA gain in various scenarios. Due to the advantages of IRS and NOMA, these two techniques have been combined recently [23]–[26]. In [23], Mu *et al*. considered a joint active and passive beamforming design problem to maximize the sum rate in IRS-aided NOMA networks. The downlink communication of IRS-assisted NOMA systems was investigated by Zuo *et al*. [24], in which the system throughput was maximized by jointly optimizing the channel assignment, SIC decoding order, power allocation, and IRS coefficients. In [25], Ding *et al*. proposed a design of IRS-assisted NOMA to guarantee the service of cell-edge users by applying IRS to align the cell-edge users channel vectors. As a further advance, an IRS enhanced millimeter-wave (mmWave) NOMA system was considered in [26], which confirms that by introducing IRS, the coverage of mmWave-NOMA systems has a significant improvement, especially when there are no direct links between the base station (BS) and users.

However, to the best of our knowledge, the security aspect of IRS-assisted NOMA networks has not been investigated. Different from NOMA, introducing IRS provides an additional reflection link that may enhance the signals received by the potential eavesdropper, especially when the eavesdropping CSI is unknown. Thus, this will be a double-edged sword for the secure transmission. Motivated by the aforementioned discussion, in this paper, we propose an artificial jamming aided IRS-NOMA scheme, in which the jamming signal is generated with NOMA information to disrupt the potential eavesdropping. The contributions of this paper are summarized as follows.

- To the best of our knowledge, research on the security of IRS-assisted NOMA networks has not been done. Thus, the first contribution of this paper is the proposal of an artificial jamming aided IRS-NOMA scheme, which could maximize the legitimate sum rate while guaranteeing the security via artificial jamming.
- In the proposed scheme, the artificial jamming is generated together with the NOMA information, which can suppress the eavesdropping efficiently. At legitimate receivers, the jamming signal can be completely eliminated via SIC with the help of the transmit beamforming and IRS reflecting optimization.
- Due to the non-convexity of the proposed optimization problem, it is first decomposed into two subproblems, i.e., optimizing the transmit beamforming vectors with fixed IRS reflecting vector and vice versa. Then, these two subproblems are approximated into convex ones via successive convex approximation (SCA) and the original problem can be solved effectively by an iterative algorithm based on alternating optimization.

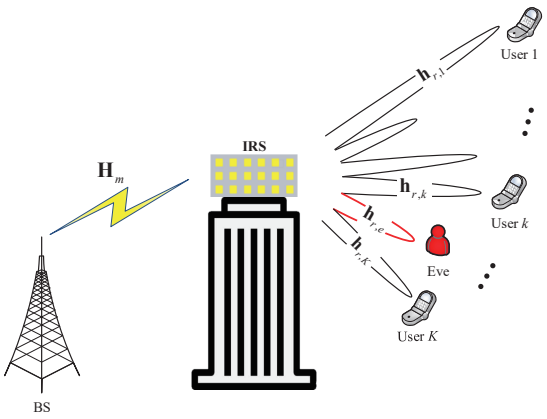

Fig. 1. Artificial jamming assisted IRS-NOMA network with multiple users and one passive eavesdropper.

The rest of this paper is organized as follows. Section II introduces the system model. The optimization problem is formulated in Section III. In Section IV, the formulated problem is first decomposed into two subproblems, and then an algorithm is proposed to solve them iteratively. In Section V, simulation results are presented, followed by conclusions in Section VI.

Notation: $\mathbb{C}^{M\times N}$ is the space of complex matrices. $\mathbb{R}^{a\times b}$ is the $a\times b$-dimensional real matrix. $\mathbf{I}_N$ is the $N\times N$ identity matrix. $\mathbf{a}^H$ and diag($\mathbf{a}$) denote the conjugate transpose and the diagonal matrix of $\mathbf{a}$, respectively. $\mathcal{CN}(\mathbf{n},\mathbf{N})$ is the complex Gaussian distribution with mean matrix $\mathbf{n}$ and covariance matrix $\mathbf{N}$. $\mathbf{A}\succeq 0$ denotes that $\mathbf{A}$ is a Hermitian positive semidefinite matrix. $\bigtriangledown_x$ denotes the gradient of the variable x, and $Re(\cdot)$ is the real operator.

II. System Model

As shown in Fig. 1, we consider the secure communication from a M-antenna BS to K single-antenna NOMA users in the presence of one passive eavesdropper, where an IRS is deployed on the facade of a surrounding building to strengthen the desired signal. The direct path between the BS and mobile users is blocked due to unfavorable propagation conditions. The kth user $U_k, k\in\mathcal{K}$ has a fixed location $(x_k, y_k, 0)$ on the ground, where $\mathcal{K}=\{1,2,\ldots,K\}$. The CSI of all the legitimate channels is assumed to be perfectly known by the BS as it can be efficiently obtained via the recent advances in channel estimation for IRS [27], [28].

Assume that a potential eavesdropper exists to collect the confidential information of legitimate users, with its CSI unavailable for the legitimate network due to its passive characteristic. To disrupt the eavesdropping and guarantee the secure transmission of legitimate users, the artificial jamming is generated together with NOMA information at the BS. The

transmitted signal can be expressed as

$$\mathbf{x} = \sum_{k\in\mathcal{K}} \mathbf{w}_k s_k + \mathbf{w}_{jam} z, \tag{1}$$

where $\mathbf{w}_k \in \mathbb{C}^{M\times 1}$ denotes the precoding vector for user k, with $\|\mathbf{w}_k\|^2 = P_k$, s_k is the NOMA information of U_k satisfying $|s_k|^2 = 1$, $\mathbf{w}_{jam} \in \mathbb{C}^{M\times 1}$ represents the artificial jamming vector with $\|\mathbf{w}_{jam}\|^2 = P_{jam}$, and z denotes the jamming signal satisfying $|z|^2 = 1$.

The received signal at the kth user can be given by

$$y_k = \mathbf{h}_{r,k}\mathbf{\Phi}\mathbf{H}_m\mathbf{x} + n_k, k \in \mathcal{K}, \tag{2}$$

where $n_k \sim \mathcal{CN}(0,\sigma^2)$ denotes the additive white Gaussian noise (AWGN) at U_k with mean zero and variance σ^2. $\mathbf{\Phi} = \text{diag}\left(e^{j\theta_1}, e^{j\theta_2}, \ldots, e^{j\theta_N}\right) \in \mathbb{C}^{N\times N}$ represents the diagonal phase-shifting matrix by all IRS reflecting elements, where N denotes the number of elements on the IRS. $\theta_n \in [0, 2\pi)$ is the phase shift on the combined incident signal by its n-th element, $\forall n = 1, 2, \ldots, N$. $\mathbf{H}_m \in \mathbb{C}^{N\times M}$ denotes the Rician channel fading matrix between the BS and the IRS, which can be given by

$$\mathbf{H}_m = \sqrt{\beta_0 d_{BI}^{-\alpha_{BI}}}\left(\sqrt{\frac{\mathcal{K}_{BI}}{\mathcal{K}_{BI}+1}}\widehat{\mathbf{G}}_L + \sqrt{\frac{1}{\mathcal{K}_{BI}+1}}\widehat{\mathbf{G}}_R\right), \tag{3}$$

where β_0 represents the path loss at the reference distance of 1 meter, d_{BI} denotes the distance from the BS to the IRS, and α_{BI} denotes the path-loss exponent. $\widehat{\mathbf{G}}_L \in \mathbb{C}^{N\times M}$ is the deterministic line-of-sight (LoS) channel component, and $\widehat{\mathbf{G}}_R \sim \mathcal{CN}(\mathbf{0}, \mathbf{I})$ denotes the scattering component. In addition, $\mathcal{K}_{BI} > 0$ is the corresponding Rician factor.

Similarly, $\mathbf{h}_{r,k} \in \mathbb{C}^{1\times N}$ is the Rician channel fading vector from the IRS to the kth user, which can be expressed as

$$\mathbf{h}_{r,k} = \sqrt{\beta_0 d_k^{-\alpha_{r,k}}}\left(\sqrt{\frac{\mathcal{K}_{IU}}{\mathcal{K}_{IU}+1}}\widehat{\mathbf{g}}_L + \sqrt{\frac{1}{\mathcal{K}_{IU}+1}}\widehat{\mathbf{g}}_R\right), \tag{4}$$

where d_k is the distance between the IRS and the kth user, $\alpha_{r,k}$ is the path-loss exponent, and $\widehat{\mathbf{g}}_L \in \mathbb{C}^{1\times N}$ and $\widehat{\mathbf{g}}_R \sim \mathcal{CN}(\mathbf{0}, \mathbf{I})$ represent the deterministic LoS channel component and the scattering component, respectively. $\mathcal{K}_{IU}$ is the corresponding Rician factor.

Without loss of generality, we assume that the channel gains between the IRS and legitimate users satisfy

$$0 < \|\mathbf{h}_{r,1}\|^2 \le \cdots \le \|\mathbf{h}_{r,K}\|^2. \tag{5}$$

Then, the transmit power from the BS satisfies

$$\sum_{k\in\mathcal{K}} \|\mathbf{w}_k\|^2 + \|\mathbf{w}_{jam}\|^2 = P_{max}, \tag{6}$$

where P_{max} denotes the maximum transmit power for BS.

For convenience, we define the IRS reflecting vector as $\mathbf{v}^H = [v_1, v_2, \ldots, v_N]$, where $v_n = \mathbf{\Phi}_{n,n} = e^{j\theta_n}, \forall n$. By changing the variables, we have

$$\mathbf{h}_{r,k}\mathbf{\Phi}\mathbf{H}_m = \mathbf{v}^H\mathbf{H}_{mrk}, \tag{7}$$

where $\mathbf{H}_{mrk} = \text{diag}(\mathbf{h}_{r,k})\mathbf{H}_m$. Therefore, the signal-to-interference-plus-noise ratio (SINR) at the kth user can be derived as

$$\gamma_k^k = \frac{\left|\mathbf{v}^H\mathbf{H}_{mrk}\mathbf{w}_k\right|^2}{\sum_{i=k+1}^{K}\left|\mathbf{v}^H\mathbf{H}_{mrk}\mathbf{w}_i\right|^2 + \left|\mathbf{v}^H\mathbf{H}_{mrk}\mathbf{w}_{jam}\right|^2 + \sigma^2}. \tag{8}$$

In NOMA systems, each receiver utilizes SIC to eliminate the multi-access interference. The SIC decoding order among users is mainly determined by the channel quality. Accordingly, the user with a stronger channel gain should first decode the messages from other users with weaker channels. However, due to the IRS, the decoding order of SIC not only depends on the transmit beamforming vectors $\{\mathbf{w}_k\}$ but also on the IRS reflecting vector $\{\mathbf{v}\}$[1]. Let $\pi(k)$ denotes the decoding order of the kth user. Then, $\pi(k) = m$ means that the message for the kth user is the m-th signal to be decoded at the receiver. According to the channel assumption in (5), we define $\pi(k) = k$. Therefore, the following constraints in the proposed IRS-NOMA scheme should be satisfied for given decoding orders as

$$\begin{aligned}&\max_l \left|\mathbf{v}^H\mathbf{H}_{mrk}\mathbf{w}_{\pi(l)}\right|^2 \le \left|\mathbf{v}^H\mathbf{H}_{mrk}\mathbf{w}_{\pi(i)}\right|^2 \le \left|\mathbf{v}^H\mathbf{H}_{mrk}\mathbf{w}_{\pi(j)}\right|^2,\\ &\quad \forall l, i, j \in \mathcal{K}, i > j, \quad i \in \mathcal{I}, \quad l \in \mathcal{T},\end{aligned} \tag{9}$$

where $\mathcal{I} = \{1, 2, \ldots, k\}, \mathcal{T} = \{k, k+1, \ldots, K\}$.

To guarantee the secure transmission for legitimate users, we assume that artificial jamming is generated together with the NOMA signals at BS, which can suppress the reception at the eavesdropper effectively. In order to avoid adverse impact on legitimate receivers, we should make the received jamming power highest at all receivers, which can be decoded and eliminated in the first step of SIC. Thus, the decoding constraints defined in (9) can be modified as

$$\begin{aligned}&\max_l \left|\mathbf{v}^H\mathbf{H}_{mrk}\mathbf{w}_{\pi(l)}\right|^2 \le \left|\mathbf{v}^H\mathbf{H}_{mrk}\mathbf{w}_{\pi(i)}\right|^2\\ &\quad \le \left|\mathbf{v}^H\mathbf{H}_{mrk}\mathbf{w}_{\pi(j)}\right|^2 \le \left|\mathbf{v}^H\mathbf{H}_{mrk}\mathbf{w}_{jam}\right|^2,\\ &\forall l, i, j \in \mathcal{K}, i > j, \quad i \in \mathcal{I}, \quad l \in \mathcal{T}.\end{aligned} \tag{10}$$

Accordingly, the jamming signal can be removed first, and the SINR in (8) can be revised as

$$\gamma_k^k = \frac{\left|\mathbf{v}^H\mathbf{H}_{mrk}\mathbf{w}_k\right|^2}{\sum_{i=k+1}^{K}\left|\mathbf{v}^H\mathbf{H}_{mrk}\mathbf{w}_i\right|^2 + \sigma^2}, k \in \mathcal{K}, k \ne K. \tag{11}$$

For user K, its desired SINR can be expressed as

$$\gamma_K^K = \frac{\left|\mathbf{v}^H\mathbf{H}_{mrK}\mathbf{w}_K\right|^2}{\sigma^2}. \tag{12}$$

Accordingly, the corresponding SINR for the lth user to

[1]The embedded IRS controller can communicate and receive the reconfiguration request from the external BS with given wired or wireless connections.

decoding the signal for the kth user can be expressed as

$$\gamma_l^k = \frac{\left|\mathbf{v}^H \mathbf{H}_{mrl} \mathbf{w}_k\right|^2}{\sum_{i=k+1}^{K} \left|\mathbf{v}^H \mathbf{H}_{mrl} \mathbf{w}_i\right|^2 + \sigma^2}, \quad 1 \le k \le K-1,\ l \in \mathcal{T}. \tag{13}$$

In NOMA networks, the SINR for the lth user to decode the kth signal should be no smaller than the target SINR of the kth user, denoted as γ_k^{tar}, $\gamma_l^k \ge \gamma_k^{tar}$ [29], [30], in order to successfully subtract the message of U_k from the received signal at U_l. Then, the target SINR of U_k can be expressed as

$$\gamma_k^{tar} = \min\{\gamma_k^k, \gamma_{k+1}^k, \ldots, \gamma_K^k\}. \tag{14}$$

Thus, the corresponding rate for the kth user can be given by

$$R_k = \log_2(1+\gamma_k^{tar}) = \log_2\left(1 + \min_{l\in\mathcal{T}} \gamma_l^k\right). \tag{15}$$

In addition, the eavesdropping SINR towards the kth user at the potential eavesdropper can be expressed as

$$\text{SINR}_e^k = \frac{\left|\mathbf{v}^H \mathbf{H}_{mre} \mathbf{w}_k\right|^2}{\sum_{i=1, i\neq k}^{K} \left|\mathbf{v}^H \mathbf{H}_{mre} \mathbf{w}_i\right|^2 + \left|\mathbf{v}^H \mathbf{H}_{mre} \mathbf{w}_{jam}\right|^2 + \sigma^2}, \tag{16}$$

where $\mathbf{H}_{mre} = \text{diag}(\mathbf{h}_{r,e})\mathbf{H}_m$ and $\mathbf{h}_{r,e}$ denotes the channel vector between the IRS and the eavesdropper, which is unavailable for the legitimate network[2]. Thus, the secrecy rate from the BS to users in bit/s/Hz can be expressed as

$$R_{sk} = \left[R_k - \log_2\left(1 + \text{SINR}_e^k\right)\right]^+, \tag{17}$$

where $[x]^+ \triangleq \max(x, 0)$. As the eavesdropping CSI is not required by the legitimate network, the proposed scheme can be also applied to the multi-eavesdropper scenario with similar performance.

III. Problem Formulation

In this section, we formulate the optimization design of the transmit beamforming, the artificial jamming vector and the IRS reflecting vector. We aim to maximize the sum rate of all users, subject to the QoS requirement, the IRS reflecting constraint, the SIC decoding condition, and the transmit power constraint. Thus, the optimization problem can be formulated as

$$\mathbf{P0}: \max_{\mathbf{w}_1, \mathbf{w}_2, \ldots, \mathbf{w}_K, \mathbf{w}_{jam}, \mathbf{v}} \sum_{k\in\mathcal{K}} R_k \tag{18a}$$

$$s.t.\ \min_l \gamma_l^k \ge r_k, l \in \mathcal{T}, \tag{18b}$$

$$\max_{k\in\mathcal{K}} \|\mathbf{w}_k\|^2 \le \|\mathbf{w}_{jam}\|^2, \tag{18c}$$

$$\sum_{k\in\mathcal{K}} \|\mathbf{w}_k\|^2 + \|\mathbf{w}_{jam}\|^2 = P_S, \tag{18d}$$

$$|v_n| = 1, n = 1, 2, \ldots, N, \tag{18e}$$

$$(10). \tag{18f}$$

[2]In this paper, the eavesdropping CSI is used to analyze the secure performance of the proposed schemes in (16) and (17) via simulation results, not for the design of the schemes.

The constraint (18b) ensures that the SINR for the lth user to decode the kth message exceeds r_k, $l \in \mathcal{T}$, where r_k denotes the QoS requirement for the kth user. (18c) guarantees the enough jamming power to disrupt the eavesdropping. (18d) is the constraint of total transmit power at BS. The constraint (18e) indicates that each IRS reflecting element only adjusts the phase shift of incident signal and does not amplify its amplitude. (18f) denotes the SIC decoding constraints.

Note that **P0** is difficult to solve due to the non-convex constraints as well as the coupled optimization variables. To solve it, we transform the objective function (18) into a more tractable form, i.e., introducing auxiliary variables $z_k \in \mathbb{R}_+, k = 1, 2, \ldots, K$, which satisfy

$$1 + \min_l \gamma_l^k \ge z_k, l \in \mathcal{T}. \tag{19}$$

Then, we have

$$\sum_{k\in\mathcal{K}} R_k = \log_2\left(\prod_{k\in\mathcal{K}} z_k\right). \tag{20}$$

Nevertheless, the maximum value of the $\log(\cdot)$ function in (20) remains hard to obtain. Thus, we can turn to find its maximum square root with all auxiliary variables $z_k (k \in \mathcal{K})$ multiplied, i.e., $\sqrt{\prod_{k\in\mathcal{K}} z_k}$, which is concave and also non-decreasing. Accordingly, (19) and (20) can be replaced by $Z \le \sqrt{\prod_{k\in\mathcal{K}} z_k}$ as another constraint in the optimization problem. Using this conversion, the original problem **P0** can be transformed as

$$\mathbf{P1}: \max_{\mathbf{w}_1, \mathbf{w}_2, \ldots, \mathbf{w}_K, \mathbf{w}_{jam}, \mathbf{v}} Z \tag{21a}$$

$$s.t.\quad Z^2 \le \prod_{k\in\mathcal{K}} z_k, \tag{21b}$$

$$z_k - 1 \le \min_l \gamma_l^k, l \in \mathcal{T}, \tag{21c}$$

$$r_k \le z_k - 1, \tag{21d}$$

$$\max_{k\in\mathcal{K}} \|\mathbf{w}_k\|^2 \le \|\mathbf{w}_{jam}\|^2, \tag{21e}$$

$$\sum_{k\in\mathcal{K}} \|\mathbf{w}_k\|^2 + \|\mathbf{w}_{jam}\|^2 = P_S, \tag{21f}$$

$$|v_n| = 1, n = 1, 2, \ldots, N, \tag{21g}$$

$$(10). \tag{21h}$$

According to [31], (21b) can be expressed as a system of second-order cone (SOC) constraints, which has no negative impact on the target function. Thus, we first define

$$z_{1,\xi}^2 \le \prod_{k=1}^{\xi} z_k, \ \ \xi \ge 2, \xi \in \mathcal{K}. \tag{22}$$

Specifically, when $\xi = K$, we have $z_{1,K} = Z$. Furthermore, involving the intermediate variables $t_{1,\xi} \in \mathbb{R}_+, \xi =$

$1, 2, \ldots, K$, the inequality (22) can be decomposed as

$$(22) \Rightarrow \begin{cases} z_{1,\xi-1}^2 \leq \prod_{k=1}^{\xi-1} z_k, \\ t_{1,\xi-1} \leq z_{1,\xi-1}^2, \\ z_{1,\xi}^2 \leq z_\xi t_{1,\xi-1}. \end{cases} \tag{23}$$

In addition, the hyperbolic constraint $w^2 \leq xy$ $(x \geq 0, y \geq 0)$ can be converted into $\left\| [2w, x-y]^H \right\| \leq x + y$. Based on the similar conversion, (23) can be reformulated into a series of SOC constraints as

$$\begin{cases} \left\| [2z_{1,2}, (z_1 - z_2)]^H \right\| \leq z_1 + z_2, \\ \left\| [2z_{1,3}, (t_{1,2} - z_3)]^H \right\| \leq t_{1,2} + z_3, \\ \ldots\ldots \\ \left\| [2z_{1,\xi}, (t_{1,\xi-1} - z_\xi)]^H \right\| \leq t_{1,\xi-1} + z_\xi. \end{cases} \tag{24}$$

By replacing the constraint (21b) with (24), (21) can be transformed to

$$\mathbf{P1}: \max_{\substack{\mathbf{w}_1, \mathbf{w}_2, \ldots, \mathbf{w}_K, \\ \mathbf{w}_{jam}, \mathbf{v}}} Z \tag{25a}$$

$$s.t. \ \left\| [2z_{1,\xi}, (t_{1,\xi-1} - z_\xi)]^H \right\| \leq t_{1,\xi-1} + z_\xi, \tag{25b}$$

$$z_k - 1 \leq \min_l \gamma_l^k, l \in \mathcal{T}, \tag{25c}$$

$$r_k \leq z_k - 1, \tag{25d}$$

$$\max_{k \in \mathcal{K}} \|\mathbf{w}_k\|^2 \leq \|\mathbf{w}_{jam}\|^2, \tag{25e}$$

$$\sum_{k \in \mathcal{K}} \|\mathbf{w}_k\|^2 + \|\mathbf{w}_{jam}\|^2 = P_S, \tag{25f}$$

$$|v_n| = 1, n = 1, 2, \ldots, N, \tag{25g}$$

$$(10). \tag{25h}$$

However, (25) is still non-convex and difficult to solve since the transmit beamforming vectors $\mathbf{w}_k$, the artificial jamming vector $\mathbf{w}_{jam}$ and the IRS reflecting vector $\mathbf{v}$ are coupled. We decompose the original problem into two subproblems of transmit beamforming optimization and IRS reflecting optimization, which can be approximated as convex ones and solved alternately in the next section.

IV. Beamforming and Reflecting Optimization

In this section, the optimization problem is decomposed into two subproblems, which can be solved by alternately optimizing the transmit beamforming vectors and IRS reflecting vector. In addition, the convergence and computational complexity of the proposed algorithm are also analyzed.

A. Beamforming Optimization

For any given IRS reflecting vector $\mathbf{v}$, (25) can be decomposed as

$$\mathbf{P2}: \max_{\substack{\mathbf{w}_1, \mathbf{w}_2, \ldots, \mathbf{w}_K, \\ \mathbf{w}_{jam}}} Z \tag{26a}$$

$$s.t. \ \left\| [2z_{1,\xi}, (t_{1,\xi-1} - z_\xi)]^H \right\| \leq t_{1,\xi-1} + z_\xi, \tag{26b}$$

$$z_k - 1 \leq \min_l \gamma_l^k, l \in \mathcal{T} \tag{26c}$$

$$r_k \leq z_k - 1, \tag{26d}$$

$$\max_{k \in \mathcal{K}} \|\mathbf{w}_k\|^2 \leq \|\mathbf{w}_{jam}\|^2, \tag{26e}$$

$$\sum_{k \in \mathcal{K}} \|\mathbf{w}_k\|^2 + \|\mathbf{w}_{jam}\|^2 = P_S, \tag{26f}$$

$$(10). \tag{26g}$$

P2 is a non-convex problem mainly due to the non-convex constraints (26c) and (10). Then, for the constraint (26c), it can be changed into

$$\begin{cases} \text{SINR}_k^k \geq z_k - 1, \\ \text{SINR}_{k+1}^k \geq z_k - 1, \\ \ldots \\ \text{SINR}_K^k \geq z_k - 1. \end{cases} \tag{27}$$

Thus, we have

$$\begin{aligned} &\frac{\left|\mathbf{v}^H \mathbf{H}_{mrl} \mathbf{w}_k\right|^2}{\sum_{i=k+1}^{K} \left|\mathbf{v}^H \mathbf{H}_{mrl} \mathbf{w}_i\right|^2 + \sigma^2} \geq z_k - 1, \\ &1 \leq k \leq K-1, \ l \in \mathcal{T}. \end{aligned} \tag{28}$$

Furthermore, it can be formulated as

$$\sum_{i=k+1}^{K} \left|\mathbf{v}^H \mathbf{H}_{mrl} \mathbf{w}_i\right|^2 \leq \frac{\left|\mathbf{v}^H \mathbf{H}_{mrl} \mathbf{w}_k\right|^2}{z_k - 1} - \sigma^2. \tag{29}$$

However, it is still non-convex and difficult to solve. To tackle this issue, we apply SCA to transform it and further introduce the Taylor series approximation. For a differentiable convex function $f(x)$, it can be approximated by its tangential function as $g(x, \bar{x})$, where $g(x, \bar{x})$ is the first order Taylor expansion around $\bar{x}$. Thus, we have

$$f(x) \geq g(x, \bar{x}) = f(\bar{x}) + \bigtriangledown_x f(\bar{x})(x - \bar{x}). \tag{30}$$

When $x = \bar{x}$, the equality holds.

Based on the above Taylor series approximation, Proposition 1 is presented to approximate (29).

Proposition 1: Define a function as

$$Q(\mathbf{w}_k, z_k) = \frac{\left|\mathbf{v}^H \mathbf{H}_{mrl} \mathbf{w}_k\right|^2}{z_k - 1} - \sigma^2. \tag{31}$$

The first order Taylor approximation to $Q(\mathbf{w}_k, z_k)$ around $(\bar{\mathbf{w}}_k, \bar{z}_k)$ can be expressed as

$$\begin{aligned} \mathcal{Q}(\mathbf{w}_k, z_k, \bar{\mathbf{w}}_k, \bar{z}_k) &= \frac{2Re(\mathbf{v}^H \mathbf{H}_{mrl} \mathbf{w}_k \bar{\mathbf{w}}_k^H \mathbf{H}_{mrl}^H \mathbf{v})}{\bar{z}_k - 1} \\ &- \frac{Re(\bar{\mathbf{w}}_k^H \mathbf{H}_{mrl}^H \mathbf{v} \mathbf{v}^H \mathbf{H}_{mrl} \bar{\mathbf{w}}_k)}{(\bar{z}_k - 1)^2}(z_k - 1) - \sigma^2. \end{aligned} \tag{32}$$

In this way, $Q(\mathbf{w}_k, z_k)$ can be replaced by $\mathcal{Q}(\mathbf{w}_k, z_k, \bar{\mathbf{w}}_k, \bar{z}_k)$.

Proof: According to the Taylor series approximation in (30), we have

$$\begin{aligned} Q(\mathbf{w}_k, z_k) \geq & Q(\bar{\mathbf{w}}_k, \bar{z}_k) + \left.\frac{\partial Q}{\partial \mathbf{w}_k}\right|_{(\bar{\mathbf{w}}_k, \bar{z}_k)} (\mathbf{w}_k - \bar{\mathbf{w}}_k) \\ & + \left.\frac{\partial Q}{\partial z_k}\right|_{(\bar{\mathbf{w}}_k, \bar{z}_k)} (z_k - \bar{z}_k) \triangleq \mathcal{Q}(\mathbf{w}_k, z_k, \bar{\mathbf{w}}_k, \bar{z}_k), \end{aligned} \tag{33}$$

where

$$\begin{aligned} \mathcal{Q}(\mathbf{w}_k, z_k, \bar{\mathbf{w}}_k, \bar{z}_k) = & \frac{\mathbf{v}^H \mathbf{H}_{mrl} \bar{\mathbf{w}}_k \bar{\mathbf{w}}_k^H \mathbf{H}_{mrl}^H \mathbf{v}}{\bar{z}_k - 1} - \sigma^2 \\ & + \frac{2\bar{\mathbf{w}}_k^H \mathbf{H}_{mrl}^H \mathbf{v}\mathbf{v}^H \mathbf{H}_{mrl}}{\bar{z}_k - 1} (\mathbf{w}_k - \bar{\mathbf{w}}_k) \\ & - \frac{\mathbf{v}^H \mathbf{H}_{mrl} \bar{\mathbf{w}}_k \bar{\mathbf{w}}_k^H \mathbf{H}_{mrl}^H \mathbf{v}}{(\bar{z}_k - 1)^2} \left[z_k - 1 - (\bar{z}_k - 1) \right]. \end{aligned} \tag{34}$$

To match with the real characteristic of the function $Q(\mathbf{w}_k, z_k)$, (34) can be further approximated as

$$\begin{aligned} \mathcal{Q}(\mathbf{w}_k, z_k, \bar{\mathbf{w}}_k, \bar{z}_k) = & \frac{2Re\left(\mathbf{v}^H \mathbf{H}_{mrl} \mathbf{w}_k \bar{\mathbf{w}}_k^H \mathbf{H}_{mrl}^H \mathbf{v}\right)}{\bar{z}_k - 1} \\ & - \frac{Re\left(\mathbf{v}^H \mathbf{H}_{mrl} \bar{\mathbf{w}}_k \bar{\mathbf{w}}_k^H \mathbf{H}_{mrl}^H \mathbf{v}\right)}{(\bar{z}_k - 1)^2} (z_k - 1) - \sigma^2 \\ = & \frac{2Re\left(\bar{\mathbf{w}}_k^H \mathbf{H}_{mrl}^H \mathbf{v}\mathbf{v}^H \mathbf{H}_{mrl} \mathbf{w}_k\right)}{\bar{z}_k - 1} \\ & - \frac{Re\left(\bar{\mathbf{w}}_k^H \mathbf{H}_{mrl}^H \mathbf{v}\mathbf{v}^H \mathbf{H}_{mrl} \bar{\mathbf{w}}_k\right)}{(\bar{z}_k - 1)^2} (z_k - 1) - \sigma^2. \end{aligned} \tag{35}$$

The approximation in (33) holds when the conditions $\mathbf{v}_k = \bar{\mathbf{v}}_k$ and $z_k = \bar{z}_k$ are satisfied.

From the above derivation, $Q(\mathbf{v}_k, z_k)$ can be approximated as $\mathcal{Q}(\mathbf{v}_k, z_k, \bar{\mathbf{v}}_k, \bar{z}_k)$, and (31) can be transformed into a convex one as (32). ∎

Nevertheless, **P2** is still non-convex due to (10), which can be regarded as a series of inequalities as

$$\left|\mathbf{v}^H \mathbf{H}_{mrk} \mathbf{w}_i\right|^2 \leq \left|\mathbf{v}^H \mathbf{H}_{mrk} \mathbf{w}_j\right|^2, \forall i, j \in \mathcal{K}, i > j. \tag{36}$$

Note that the right sides of these inequalities are quadratic functions of $\mathbf{w}_j$, which can be linearized using the following proposition.

Proposition 2: Define a function as

$$F(\mathbf{w}_j) = \left|\mathbf{v}^H \mathbf{H}_{mrk} \mathbf{w}_j\right|^2, j \in \mathcal{K}. \tag{37}$$

The first order Taylor approximation to $F(\mathbf{w}_j)$ at a tangent point $\bar{\mathbf{w}}_j$ can be expressed as

$$\begin{aligned} \mathcal{F}(\mathbf{w}_j, \bar{\mathbf{w}}_j) = & 2Re\left(\bar{\mathbf{w}}_j^H \mathbf{H}_{mrk}^H \mathbf{v}\mathbf{v}^H \mathbf{H}_{mrk} \mathbf{w}_j\right) \\ & - Re\left(\bar{\mathbf{w}}_j^H \mathbf{H}_{mrk}^H \mathbf{v}\mathbf{v}^H \mathbf{H}_{mrk} \bar{\mathbf{w}}_j\right). \end{aligned} \tag{38}$$

In this way, (37) can be replaced by (38), and the constraint (10) can be approximated as a convex one.

Proof: According to the Taylor series approximation, (37) is a differentiable convex function, which satisfies

$$F(\mathbf{w}_j) \geq F(\bar{\mathbf{w}}_j) + \bigtriangledown F(\bar{\mathbf{w}}_j)^H (\mathbf{w}_j - \bar{\mathbf{w}}_j). \tag{39}$$

Substituting (37) into this inequality (39) based on the law of derivation, we have

$$\begin{aligned} F(\mathbf{w}_j) \geq & \mathbf{v}^H \mathbf{H}_{mrk} \bar{\mathbf{w}}_j \bar{\mathbf{w}}_j^H \mathbf{H}_{mrk}^H \mathbf{v} \\ & + 2\mathbf{v}^H \mathbf{H}_{mrk} \bar{\mathbf{w}}_j^H \mathbf{H}_{mrk}^H \mathbf{v} (\mathbf{w}_j - \bar{\mathbf{w}}_j). \end{aligned} \tag{40}$$

When $\bar{\mathbf{w}}_j \bar{\mathbf{w}}_j^H \succeq 0$ and $\mathbf{v}^H \mathbf{H}_{mrk} \mathbf{H}_{mrk}^H \mathbf{v} \succeq 0$, we can obtain

$$F(\mathbf{w}_j) \triangleq \mathcal{F}(\mathbf{w}_j, \bar{\mathbf{w}}_j). \tag{41}$$

From the above derivation, $F(\mathbf{w}_j)$ can be approximated as $\mathcal{F}(\mathbf{w}_j, \bar{\mathbf{w}}_j)$. ∎

Accordingly, we keep the real part of $\mathcal{F}(\mathbf{w}_j, \bar{\mathbf{w}}_j)$, and all the similar inequalities in (10) can be approximated into convex ones as

$$\begin{aligned} \left|\mathbf{v}^H \mathbf{H}_{mrk} \mathbf{w}_i\right|^2 \leq & 2Re\left(\bar{\mathbf{w}}_j^H \mathbf{H}_{mrk}^H \mathbf{v}\mathbf{v}^H \mathbf{H}_{mrk} \mathbf{w}_j\right) \\ & - Re\left(\bar{\mathbf{w}}_j^H \mathbf{H}_{mrk}^H \mathbf{v}\mathbf{v}^H \mathbf{H}_{mrk} \bar{\mathbf{w}}_j\right), \end{aligned} \tag{42}$$

which can be guaranteed when $\mathbf{w}_j = \bar{\mathbf{w}}_j$ holds.

Specifically, when $\mathbf{w}_j = \mathbf{w}_{jam}$, the right-hand side of (10) can be converted as

$$\begin{aligned} \left|\mathbf{v}^H \mathbf{H}_{mrk} \mathbf{w}_1\right|^2 \leq & 2Re\left(\bar{\mathbf{w}}_{jam}^H \mathbf{H}_{mrk}^H \mathbf{v}\mathbf{v}^H \mathbf{H}_{mrk} \mathbf{w}_{jam}\right) \\ & - Re\left(\bar{\mathbf{w}}_{jam}^H \mathbf{H}_{mrk}^H \mathbf{v}\mathbf{v}^H \mathbf{H}_{mrk} \bar{\mathbf{w}}_{jam}\right). \end{aligned} \tag{43}$$

Thus, (10) can be replaced by (42) and (43), which are approximated as convex ones.

Similarly, the constraint (26e) can be expressed as

$$\begin{aligned} \max_{k \in \mathcal{K}} \|\mathbf{w}_k\|^2 \leq & \|\mathbf{w}_{jam}\|^2 \\ \triangleq & 2Re\left(\mathbf{w}_{jam}^H \bar{\mathbf{w}}_{jam}\right) - Re\left(\bar{\mathbf{w}}_{jam}^H \bar{\mathbf{w}}_{jam}\right). \end{aligned} \tag{44}$$

Using the above-mentioned approximations, **P2** can be formulated as (45) at the top of this page, which is a convex problem and can be solved easily by the existing toolbox such as CVX.

B. IRS Reflecting Optimization

For any given beamforming vectors $\mathbf{w}_1$, $\mathbf{w}_2$, …, $\mathbf{w}_K$ and $\mathbf{w}_{jam}$, the optimization problem (25) can be transformed as

$$\mathbf{P3}: \max_{\mathbf{v}} \ Z \tag{46a}$$

$$s.t. \ \left\| [2z_{1,\xi}, (t_{1,\xi-1} - z_\xi)]^H \right\| \leq t_{1,\xi-1} + z_\xi, \tag{46b}$$

$$z_k - 1 \leq \min_l \gamma_l^k, l \in \mathcal{T}, \tag{46c}$$

$$r_k \leq z_k - 1, \tag{46d}$$

$$|v_n| = 1, n = 1, 2, \ldots, N, \tag{46e}$$

$$(10). \tag{46f}$$

P3 cannot be solved directly due to the non-convex constraints (46c) and (10). Similar to (28), the constraint (46c) can be transformed as

$$\begin{aligned} & \frac{\left|\mathbf{v}^H \mathbf{H}_{mrl} \mathbf{w}_k\right|^2}{\sum_{i=k+1}^{K} \left|\mathbf{v}^H \mathbf{H}_{mrl} \mathbf{w}_i\right|^2 + \sigma^2} \geq z_k - 1, \\ & 1 \leq k \leq K - 1, \ l \in \mathcal{T}. \end{aligned} \tag{47}$$

$$
\begin{aligned}
&\max_{\mathbf{w}_1,\mathbf{w}_2,\ldots,\mathbf{w}_K,\atop \bar{\mathbf{w}}_{jam}} Z\\
&\quad s.t.\ \ r_k \le z_k - 1, k \in \mathcal{K},\\
&\qquad \left\|\left[2z_{1,\xi}, (t_{1,\xi-1} - z_\xi)\right]^H\right\| \le t_{1,\xi-1} + z_\xi, \xi \ge 2, \xi \in \mathcal{K},\\
&\qquad \begin{cases} \left\|\left[2\mathbf{v}^H\mathbf{H}_{mrl}\mathbf{w}_{k+1}, \ldots, 2\mathbf{v}^H\mathbf{H}_{mrl}\mathbf{w}_K, (\mathcal{Q}_k - 1)\right]^H\right\| \le \mathcal{Q}_k + 1,\ k = 1, 2, \ldots, K-1,\\ 0 \le \mathcal{Q}_K,\ k = K,\ \ l \in \mathcal{T}, \end{cases}\\
&\qquad \max_{k\in\mathcal{K}} \|\mathbf{w}_k\|^2 \le \|\mathbf{w}_{jam}\|^2 \triangleq 2Re\left(\mathbf{w}_{jam}^H \bar{\mathbf{w}}_{jam}\right) - Re\left(\bar{\mathbf{w}}_{jam}^H \bar{\mathbf{w}}_{jam}\right),\\
&\qquad \left|\mathbf{v}^H\mathbf{H}_{mrk}\mathbf{w}_i\right|^2 \le 2Re\left(\bar{\mathbf{w}}_j^H\mathbf{H}_{mrk}^H\mathbf{v}\mathbf{v}^H\mathbf{H}_{mrk}\mathbf{w}_j\right) - Re\left(\bar{\mathbf{w}}_j^H\mathbf{H}_{mrk}^H\mathbf{v}\mathbf{v}^H\mathbf{H}_{mrk}\bar{\mathbf{w}}_j\right), \forall i, j \in \mathcal{K}, i > j,\\
&\qquad \left|\mathbf{v}^H\mathbf{H}_{mrk}\mathbf{w}_1\right|^2 \le 2Re\left(\bar{\mathbf{w}}_{jam}^H\mathbf{H}_{mrk}^H\mathbf{v}\mathbf{v}^H\mathbf{H}_{mrk}\mathbf{w}_{jam}\right) - Re\left(\bar{\mathbf{w}}_{jam}^H\mathbf{H}_{mrk}^H\mathbf{v}\mathbf{v}^H\mathbf{H}_{mrk}\bar{\mathbf{w}}_{jam}\right),\\
&\qquad \left\|\left[\mathbf{w}_1^H, \mathbf{w}_2^H, \ldots, \mathbf{w}_K^H, \mathbf{w}_{jam}^H\right]^H\right\| = \sqrt{P_S}.
\end{aligned} \tag{45}
$$

$$
\begin{aligned}
&\max_{\mathbf{v}}\ \ Z\\
&s.t.\ \ r_k \le z_k - 1, k \in \mathcal{K},\\
&\qquad \left\|\left[2z_{1,\xi}, (t_{1,\xi-1} - z_\xi)\right]^H\right\| \le t_{1,\xi-1} + z_\xi, \xi \ge 2, \xi \in \mathcal{K},\\
&\qquad \begin{cases} \left\|\left[2\mathbf{w}_{k+1}^H\mathbf{H}_{mrl}^H\mathbf{v}, \ldots, 2\mathbf{w}_K^H\mathbf{H}_{mrl}^H\mathbf{v}, (\mathcal{G}_k - 1)\right]^H\right\| \le \mathcal{G}_k + 1,\ k = 1, 2, \ldots, K-1,\\ 0 \le \mathcal{G}_K,\ k = K,\ \ l \in \mathcal{T}, \end{cases}\\
&\qquad 0 \le |v_n| \le 1, n = 1, 2, \ldots, N,\\
&\qquad \left|\mathbf{w}_i^H\mathbf{H}_{mrk}^H\mathbf{v}\right|^2 \le 2Re\left(\bar{\mathbf{v}}^H\mathbf{H}_{mrk}^H\mathbf{w}_j\mathbf{w}_j^H\mathbf{H}_{mrk}\mathbf{v}\right) - Re\left(\bar{\mathbf{v}}^H\mathbf{H}_{mrk}^H\mathbf{w}_j\mathbf{w}_j^H\mathbf{H}_{mrk}\bar{\mathbf{v}}\right), \forall i, j \in \mathcal{K}, i > j,\\
&\qquad \left|\mathbf{w}_1^H\mathbf{H}_{mrk}^H\mathbf{v}\right|^2 \le 2Re\left(\bar{\mathbf{v}}^H\mathbf{H}_{mrk}^H\mathbf{w}_{jam}\mathbf{v}_k^H\mathbf{H}_{mrk}\mathbf{v}\right) - Re\left(\bar{\mathbf{v}}^H\mathbf{H}_{mrk}^H\mathbf{w}_{jam}\mathbf{w}_{jam}^H\mathbf{H}_{mrk}\bar{\mathbf{v}}\right).
\end{aligned} \tag{60}
$$

Under the given beamforming vectors $\mathbf{w}_k$ and $\mathbf{w}_{jam}$, we can conclude that

$$
\left|\mathbf{v}^H\mathbf{H}_{mrl}\mathbf{w}_k\right|^2 = \left|(\mathbf{H}_{mrl}\mathbf{w}_k)^H\mathbf{v}\right|^2 = \left|\mathbf{w}_k^H\mathbf{H}_{mrl}^H\mathbf{v}\right|^2. \tag{48}
$$

Thus, (47) can be converted into

$$
\begin{aligned}
&\frac{\left|\mathbf{w}_k^H\mathbf{H}_{mrl}^H\mathbf{v}\right|^2}{\sum_{i=k+1}^{K}\left|\mathbf{w}_i^H\mathbf{H}_{mrl}^H\mathbf{v}\right|^2 + \sigma^2} \ge z_k - 1,\\
&\quad 1 \le k \le K-1,\ l \in \mathcal{T}.
\end{aligned} \tag{49}
$$

Furthermore, it can be formulated as

$$
\sum_{i=k+1}^{K}\left|\mathbf{w}_i^H\mathbf{H}_{mrl}^H\mathbf{v}\right|^2 \le \frac{\left|\mathbf{w}_k^H\mathbf{H}_{mrl}^H\mathbf{v}\right|^2}{z_k - 1} - \sigma^2. \tag{50}
$$

Similarly, due to the non-convexity of (50), we apply SCA via Proposition 3 to transform it.

Proposition 3: Define a function as

$$
G(\mathbf{v}, z_k) = \frac{\left|\mathbf{w}_k^H\mathbf{H}_{mrl}^H\mathbf{v}\right|^2}{z_k - 1} - \sigma^2. \tag{51}
$$

Then, according to the Taylor series approximation, it can be approximated as

$$
\begin{aligned}
\mathcal{G}(\mathbf{v}, z_k, \bar{\mathbf{v}}, \bar{z}_k) &= \frac{2Re\left(\bar{\mathbf{v}}^H\mathbf{H}_{mrl}\mathbf{w}_k\mathbf{w}_k^H\mathbf{H}_{mrl}\mathbf{v}\right)}{\bar{z}_k - 1}\\
&- \frac{Re\left(\mathbf{w}_k^H\mathbf{H}_{mrl}^H\bar{\mathbf{v}}\bar{\mathbf{v}}^H\mathbf{H}_{mrl}\mathbf{w}_k\right)}{(\bar{z}_k - 1)^2}(z_k - 1) - \sigma^2.
\end{aligned} \tag{52}
$$

In this way, $G(\mathbf{v}, z_k)$ can be replaced by $\mathcal{G}(\mathbf{v}, z_k, \bar{\mathbf{v}}, \bar{z}_k)$.

Proof: According to the Taylor series approximation in (30), we have

$$
\begin{aligned}
G(\mathbf{v}, z_k) \ge& G(\bar{\mathbf{v}}, \bar{z}_k) + \left.\frac{\partial G}{\partial \mathbf{v}}\right|_{(\bar{\mathbf{v}}, \bar{z}_k)}(\mathbf{v} - \bar{\mathbf{v}})\\
&+ \left.\frac{\partial G}{\partial z_k}\right|_{(\bar{\mathbf{v}}, \bar{z}_k)}(z_k - \bar{z}_k) \triangleq \mathcal{G}(\mathbf{v}, z_k, \bar{\mathbf{v}}, \bar{z}_k),
\end{aligned} \tag{53}
$$

where

$$
\begin{aligned}
\mathcal{G}(\mathbf{v}, z_k, \bar{\mathbf{v}}, \bar{z}_k) &= \frac{\mathbf{w}_k^H\mathbf{H}_{mrl}^H\bar{\mathbf{v}}\bar{\mathbf{v}}^H\mathbf{H}_{mrl}\mathbf{w}_k}{\bar{z}_k - 1} - \sigma^2\\
&+ \frac{2\bar{\mathbf{v}}^H\mathbf{H}_{mrl}\mathbf{w}_k\mathbf{w}_k^H\mathbf{H}_{mrl}^H}{\bar{z}_k - 1}(\mathbf{v} - \bar{\mathbf{v}})\\
&- \frac{\mathbf{w}_k^H\mathbf{H}_{mrl}^H\bar{\mathbf{v}}\bar{\mathbf{v}}^H\mathbf{H}_{mrl}\mathbf{w}_k}{(\bar{z}_k - 1)^2}\left[z_k - 1 - (\bar{z}_k - 1)\right].
\end{aligned} \tag{54}
$$

Then, it can be further expressed as

$$
\begin{aligned}
\mathcal{G}(\mathbf{v}, z_k, \bar{\mathbf{v}}, \bar{z}_k) &= \frac{2Re\left(\bar{\mathbf{v}}^H\mathbf{H}_{mrl}\mathbf{w}_k\mathbf{w}_k^H\mathbf{H}_{mrl}\mathbf{v}\right)}{\bar{z}_k - 1}\\
&- \frac{Re\left(\mathbf{w}_k^H\mathbf{H}_{mrl}^H\bar{\mathbf{v}}\bar{\mathbf{v}}^H\mathbf{H}_{mrl}\mathbf{w}_k\right)}{(\bar{z}_k - 1)^2}(z_k - 1) - \sigma^2 = (52).
\end{aligned} \tag{55}
$$

The approximation in (53) holds with the conditions $\mathbf{v} = \bar{\mathbf{v}}$ and $z_k = \bar{z}_k$ satisfied.

From the above derivation, $G(\mathbf{v}, z_k)$ can be approximated into $\mathcal{G}(\mathbf{v}, z_k, \bar{\mathbf{v}}, \bar{z}_k)$, and (51) can be transformed into a convex one as (52). ■

However, **P3** is still non-convex due to (10). Following the conversion in (48), the decoding conditions in (10) can be formulated as

$$\begin{aligned}\max_{l}\left|\mathbf{w}_l^H\mathbf{H}_{mrk}^H\mathbf{v}\right|^2 &\le \left|\mathbf{w}_{\pi(i)}^H\mathbf{H}_{mrk}^H\mathbf{v}\right|^2 \\ &\le \left|\mathbf{w}_{\pi(j)}^H\mathbf{H}_{mrk}^H\mathbf{v}\right|^2 \le \left|\mathbf{w}_{jam}^H\mathbf{H}_{mrk}^H\mathbf{v}\right|^2, \\ \forall l,i,j\in\mathcal{K}, i>j,&\quad i\in\mathcal{I},\quad l\in\mathcal{T}.\end{aligned} \tag{56}$$

For convenience, we consider (56) as a series of inequalities as

$$\left|\mathbf{w}_i^H\mathbf{H}_{mrk}^H\mathbf{v}\right|^2 \le \left|\mathbf{w}_j^H\mathbf{H}_{mrk}^H\mathbf{v}\right|^2,\quad i,j\in\mathcal{K}, i>j. \tag{57}$$

Accordingly, the inequalities in (57) can be transformed into convex ones via the same approximation as Proposition 2.

$$\begin{aligned}\left|\mathbf{w}_i^H\mathbf{H}_{mrk}^H\mathbf{v}\right|^2 \le& 2Re\big(\bar{\mathbf{v}}^H\mathbf{H}_{mrk}^H\mathbf{w}_j\mathbf{w}_j^H\mathbf{H}_{mrk}\mathbf{v}\big) \\ &-Re\big(\bar{\mathbf{v}}^H\mathbf{H}_{mrk}^H\mathbf{w}_j\mathbf{w}_j^H\mathbf{H}_{mrk}\bar{\mathbf{v}}\big).\end{aligned} \tag{58}$$

Sepcifically, when $\mathbf{w}_j=\mathbf{w}_{jam}$, the right-hand side of (56) can be converted as

$$\begin{aligned}\left|\mathbf{w}_1^H\mathbf{H}_{mrk}^H\mathbf{v}\right|^2 \le& 2Re\big(\bar{\mathbf{v}}^H\mathbf{H}_{mrk}^H\mathbf{w}_{jam}\mathbf{w}_{jam}^H\mathbf{H}_{mrk}\mathbf{v}\big) \\ &-Re\big(\bar{\mathbf{v}}^H\mathbf{H}_{mrk}^H\mathbf{w}_{jam}\mathbf{w}_{jam}^H\mathbf{H}_{mrk}\bar{\mathbf{v}}\big).\end{aligned} \tag{59}$$

As a result, all the non-convex constraints has been transformed into convex ones, and **P3** can be transformed into a convex one as (60) at the top of next page and efficiently solved via CVX.

C. Alternating Algorithm

In Section IV-A and Section IV-B, the original problem (21) has been transformed and approximated into two convex subproblems, i.e., (45) and (60). Next, we propose an iterative algorithm based on alternating optimization to solve them, which can be summarized in Algorithm 1.

Algorithm 1 Alternating Algorithm for (21)

1: Randomly initialize the reflecting vector $\mathbf{v}^{(0)}$ and the transmit beamforming vectors $\mathbf{w}_k^{(0)}, k=1,2,\ldots,K$, and $\mathbf{w}_{jam}^{(0)}$. Set the index of iteration $t=1$.
2: **Repeat**
3: For $\mathbf{v}^r$, solve (45) via CVX and obtain the optimal values $\mathbf{w}_k^{(t+1)}$ and $\mathbf{w}_{jam}^{(t+1)}$.
4: Using $\mathbf{w}_k^{(t+1)}$ and $\mathbf{w}_{jam}^{(t+1)}$, solve (60) via CVX and obtain the optimal value $\mathbf{v}^{t+1}$.
5: $t=t+1$.
6: **Until** $|Z^{(t)}-Z^{(t-1)}|$ converges.

For given $\{\mathbf{v}^r,\mathbf{w}_k^r,\mathbf{w}_{jam}^r\}$, the solution $\{\mathbf{v}^r,\mathbf{w}_k^{r+1},\mathbf{w}_{jam}^{r+1}\}$ obtained in the $(r+1)$th iteration by solving (45) is locally optimal and the objective function is non-decreasing with iterations. In the scheme, the objective function in (45) obtained by Step 3 in Algorithm 1 is a lower bound to that of its original problem (26). Similarly, the objective function in (60) is also a lower bound to that of its original problem (46). Due to the convexity of (45) and (60), each subproblem can be solved to obtain a unique solution in each iteration. Furthermore, the objective value of (60) is upper bounded by a finite value. Therefore, Algorithm 1 can be guaranteed to converge to at least a local optimal solution.

The initial reflecting vector $\mathbf{v}^{(0)}$, the transmit beamforming vectors $\mathbf{w}_k^{(0)}, k=1,2,\ldots,K$, and $\mathbf{w}_{jam}^{(0)}$ in Algorithm 1 can be generated as follows.

- **IRS Reflecting Initialization**: In the first step of Algorithm 1, the phase shift of each element is arbitrarily distributed between $[0,2\pi)$, while the reflecting amplitude is always equal to 1.
- **Transmit Beamforming Initialization**: In order to guarantee that the artificial jamming can be eliminated in the first step of SIC, the initial power allocation weight of jamming vector $\mathbf{w}_{jam}^{(0)}$ can be set to $\frac{1}{2}$, and the weights of beamforming vectors $\mathbf{w}_k^{(0)}, k=1,2,\ldots,K$, are generated with $\frac{1}{2(k+1)}$, which is helpful to satisfy the constraints in (21).

After Algorithm 1, the phase shift on the combined incident signal by its n-th element of IRS can be calculated by

$$\theta_n=\arctan\frac{Im(v_n)}{Re(v_n)}, \theta_n\in[0,2\pi), \tag{61}$$

where $Im(\cdot)$ and $Re(\cdot)$ are the imaginary operator and the real operator, respectively.

D. Computational Complexity Analysis

The main computational complexity of Algorithm 1 lies in solving **P2** and **P3**. According to [31], we can know that the computational complexity for the second-order cone programming (SOCP) is normally determined by the number of variables, constraints and its dimensions. To solve **P2**, the number of constraints in (45) can be expressed as $(1.5K^2+3.5K)$. Thus, the total number of iterations to reduce the duality gap to a threshold can be upper bounded by $\mathcal{O}\left(\sqrt{1.5K^2+3.5K}\right)$. The number of variables and dimensions for all constraints in (45) are calculated as $\left(K^2+2K+1+2(K+1)M\right)$ and $\left(4K^2+5K+(K+1)M\right)$, respectively. Therefore, the computational complexity of solving **P2** for (45) can be obtained as

$$\begin{aligned}\mathcal{O}\Big(&T_{P2}\sqrt{1.5K^2+3.5K}\left(K^2+2K+1+2(K+1)M\right)^2 \\ &\times\left(4K^2+6K+1+(K+1)M\right)\Big),\end{aligned} \tag{62}$$

where T_{P2} denotes the number of iterations. Similarly, denoting the number of iterations required for solving **P3** by T_{P3}, the corresponding complexity can be given by

$$\mathcal{O}\Big(T_{P3}\sqrt{1.5K^2+2.5K}\big(K^2+K+1+2N\big)^2\big(4K^2+6K\big)\Big). \tag{63}$$

Therefore, the overall complexity of solving (21) can be expressed as (64) at the top of next page, where T_{AO} is the number of iterations required for Algorithm 1 to converge.

V. Simulation Results and Discussion

In this section, simulation results are presented to show the performance of the proposed artificial jamming assisted IRS-NOMA scheme. Set $\alpha_{BI}=\alpha_{r,k}=2.2$, $\beta=-30$ dB,

$$\mathcal{O}\Bigg(T_{AO}\Big(T_{P2}\sqrt{1.5K^2+3.5K}\left(K^2+2K+1+2(K+1)M\right)^2\left(4K^2+6K+1+(K+1)M\right) \\ +T_{P3}\sqrt{1.5K^2+2.5K}\left(K^2+K+1+2N\right)^2\left(4K^2+6K\right)\Big)\Bigg). \tag{64}$$

$r_k = 1$, $\sigma^2 = -110$ dBm and $M = 4$. The Rician factors are $\mathcal{K}_{BI} = \mathcal{K}_{IU} = 3$ dB [23]. The BS and the IRS are set at $(5, 0, 0)$ and $(0, 50, 20)$ in meters, respectively. The legitimate users are arbitrarily distributed on the ground near the IRS, i.e., in a circle region centered at $(5, 50, 0)$ with the radius of 5 meters, and the eavesdropper is located at $(2, 50, 0)$. In practical NOMA systems, the number of users to be served should not be large to mitigate the imperfect SIC and reduce the computational complexity. Thus, we set $K = 2$ or $K = 3$. Furthermore, the scheme with random phase shift θ and the scheme without jamming are presented as benchmarks.

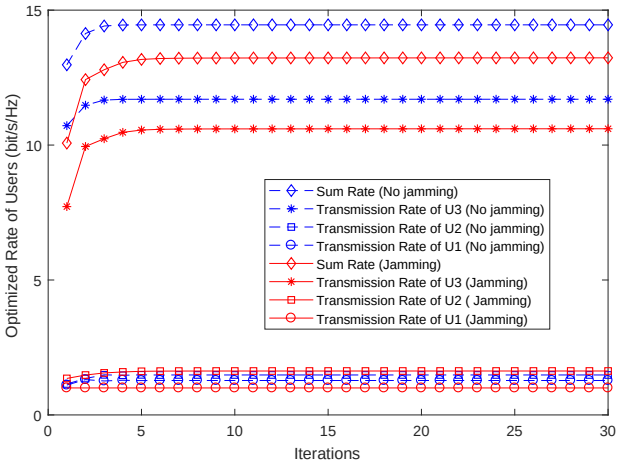

Fig. 2. The optimized transmission rate R_k and sum rate R_{sum} with iterations for three users. $M = 4$, $N = 30$, $r_k = 1$ and $P_S = 30$ dBm.

As shown in Fig. 2, we first present the convergence of Algorithm 1 for $K = 3$, $N = 30$, $r_k = 1$ and $P_S = 30$ dBm. From Fig. 2, we can observe that the proposed iterative algorithm converges quickly, i.e., within 5 to 10 iterations, which proves the stability and feasibility of Algorithm 1.

To discuss the relationship between the optimized transmit power of users and the jamming power with different QoS thresholds and different number of elements on the IRS, a two-user case in the proposed IRS-NOMA scheme is first presented in Fig. 3 and Fig. 4. Fig. 3 shows the comparison on the optimized P_{jam} and the allocated power of U_2 with different values of P_S and r_k. Set $M = 4$ and $N = 30$. From the results, we can see that the optimized P_{jam} increases with P_S. Especially, when r_k increases, the optimized jamming power also increases, i.e., P_{jam} with $r_k = 8$ is higher than P_{jam} with $r_k = 1$, while the allocated power P_2 with $r_k = 8$ is much lower. This indicates that when P_S is fixed, the far user U_1 should be allocated more power to satisfy the higher r_k. According to (18c), the jamming power should be higher than the transmit power for users to be successfully eliminated via SIC, which also results in higher P_{jam}. Thus, P_1 and P_{jam}

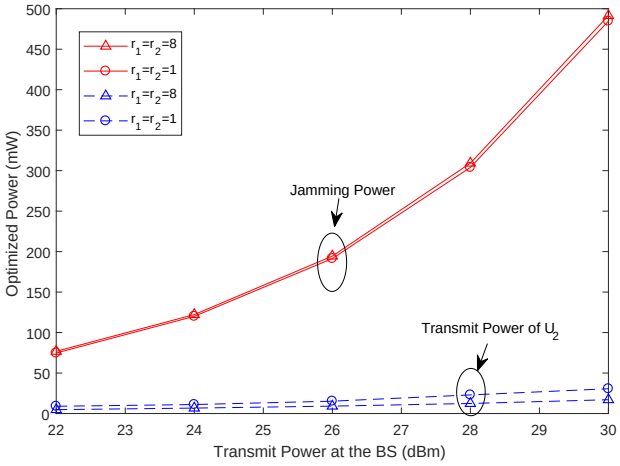

Fig. 3. Optimized jamming power P_{jam} with different values of P_S and r_k for two users. $M = 4$ and $N = 30$.

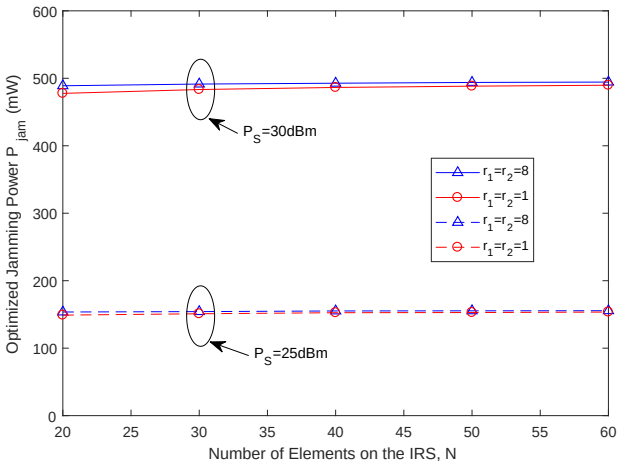

Fig. 4. Optimized jamming power P_{jam} with different values of N and r_k for two users. $M = 4$.

increase while P_2 decreases, giving a lower P_2 when $r_k = 8$ than when $r_k = 1$.

In Fig. 4, we present the optimized jamming power P_{jam} versus different values of N and r_k for the two-user case with $P_S = 25$dBm and $P_S = 30$dBm, respectively. From the results, we can observe that P_{jam} increases slightly with the growth of N, and the optimized P_{jam} with larger r_k is always higher than the P_{jam} with smaller r_k, which is consistent with the results in Fig. 3. It indicates that a larger number of IRS elements provide a more configurable link, which can reduce power consumption to satisfy the QoS requirement. Thus, more power can be allocated to generate the jamming signal.

For performance comparison, we consider a benchmark scheme, i.e., the scheme with random phase shift θ, which

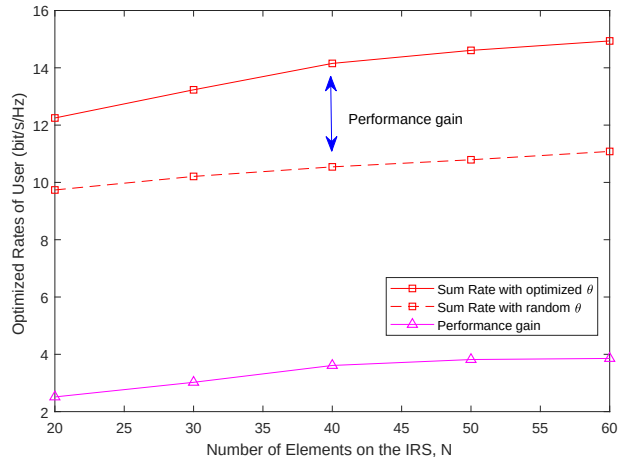

Fig. 5. The optimized sum rate of the proposed scheme and the scheme with random phase shift θ. $M = 4$, $r_k = 1$ and $P_S = 30$ dBm.

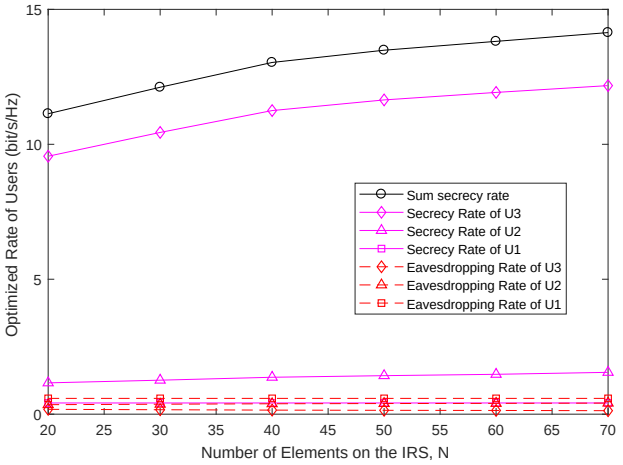

Fig. 6. The optimized secrecy rate, sum secrecy rate and eavesdropping rate with different N for three users. $M = 4$, $r_k = 1$ and $P_S = 30$ dBm.

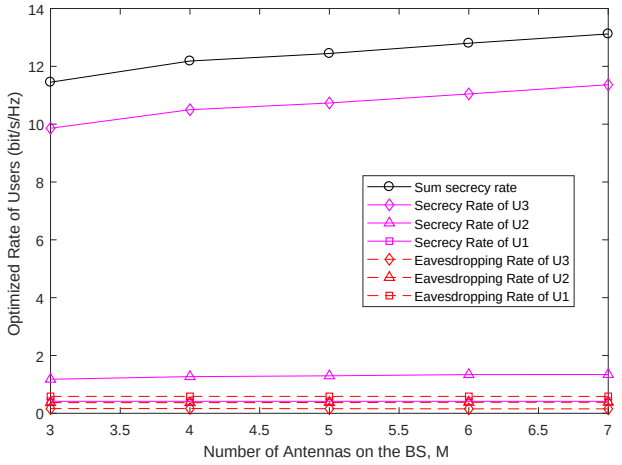

Fig. 7. The optimized secrecy rate, sum secrecy rate and eavesdropping rate of the proposed scheme with different M for three users. $N = 30$, $r_k = 1$ and $P_S = 30$ dBm.

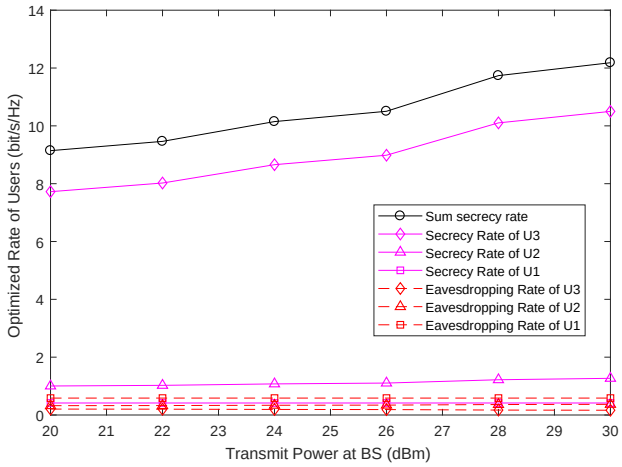

Fig. 8. The optimized secrecy rate, sum secrecy rate and eavesdropping rate of the proposed scheme with different P_S for three users. $M = 4$, $N = 30$ and $r_k = 1$.

shows the performance of the proposed IRS-NOMA scheme by setting random phase shift θ at the IRS. From the results in Fig. 5, we can observe that the sum rate in the two schemes both increases with N, since more configurable links and a higher array gain can be achieved with a lager number of IRS elements. In addition, it is worth noticing that the performance of the proposed scheme clearly outperforms the scheme with random θ. Especially, when the number of N increases, the gap between the proposed scheme and the random θ scheme is gradually widening, which demonstrates the significant array gain achieved by the transmit beamforming and IRS reflecting optimization.

To further evaluate the performance of the proposed IRS-NOMA scheme, we compare the secrecy rate, the sum secrecy rate, and the eavesdropping rate for three users with different number of elements on the IRS N in Fig. 6. From the results, it can be observed that the sum secrecy rate of all users increases with N, which is consistent with the results from Fig. 5. In addition, the nearest user U_3 has the highest secrecy rate due to its best channel gain and lowest eavesdropping rate. Accordingly, Fig. 7 presents the achievable rate versus the number of antennas at the BS M for $K = 3$, $N = 30$, $r_k = 1$ and $P_S = 30$ dBm. From Fig. 7, we can conclude that the sum secrecy rate of all users increases with M as larger beamforming gain can be achieved. In Fig. 8, we compare the optimized secrecy rate, sum secrecy rate and eavesdropping rate with different P_S. $K = 3$, $M = 4$, $N = 30$ and $r_k = 1$. From Fig. 8, we can see that the sum secrecy rate increases with P_S. Specifically, the secrecy rate of U_3 is the highest, while the secrecy rate of U_1 is the lowest, which is reasonable given the predefined relationship of channel gains. Nevertheless, the eavesdropping rate of U_1 is still a little higher, which can be further reduced by increasing the proportion of artificial jamming in beamforming vectors.

In order to present the improvement of secrecy performance with artificial jamming, we further compare the eavesdropping rate, the transmission rate and the sum rate with $P_S = 20$dBm (i.e., Fig. 9(A)-(B)) and $P_S = 30$dBm (i.e., Fig. 9(C)-(D)), respectively. Furthermore, the scheme without jamming is used as a benchmark. $K = 3$, $M = 4$, $N = 30$ and $r_k = 1$. From Fig. 9, we can see that the eavesdropping rate of all users in the proposed scheme can be reduced by artificial jamming

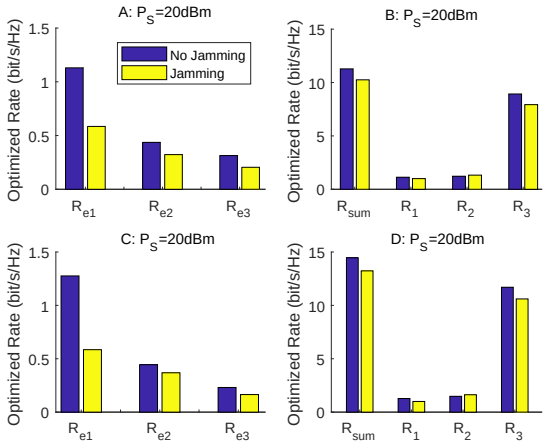

Fig. 9. Comparison on eavesdropping rate, secrecy rate and sum secrecy rate of the proposed IRS-NOMA scheme and the scheme without jamming with different P_S. $K = 3$, $M = 4$, $N = 30$ and $r_k = 1$.

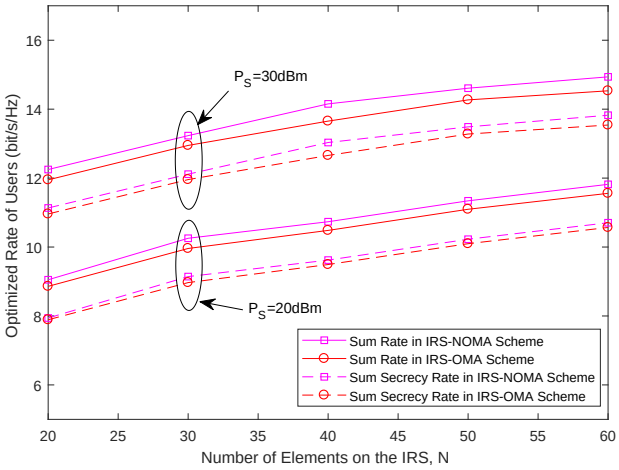

Fig. 10. The optimized sum rate and sum secrecy rate of the proposed IRS-NOMA scheme and the IRS-OMA scheme with different values of N and P_S. $K = 3$, $M = 4$ and $r_k = 1$.

compared to that of the scheme without jamming. Particularly, the eavesdropping rate towards U_1 is disrupted effectively. It is worth noticing that U_1 has the worst channel quality and is most threatened by the potential eavesdropper, due to its highest transmit power according to NOMA. On the other hand, there is a little difference in the achievable transmission rate between the proposed scheme and the scheme without jamming. Especially when P_S is lower, i.e., $P_S = 20$ dBm in Fig. 9(B), we can see that the achievable transmission rate in the proposed scheme is decreased compared to that of the scheme without jamming. However, this influence can be prevented by increasing P_S, as shown in Fig. 9(D), i.e., when $P_S = 30$ dBm, the achievable R_{sum} is only a little lower compared with the benchmark scheme.

The comparison on the proposed IRS-assisted NOMA scheme and the IRS-assisted OMA scheme is presented in Fig. 10. In the IRS-assisted OMA scheme, the BS serves three users through the frequency division multiple access, with the unit bandwidth equally divided. Similar to the NOMA scheme, the sum rate for the OMA users is maximized by optimizing the transmit beamforming together with the artificial jamming vector and the IRS reflecting vector, subject to the QoS requirement and the transmit power constraint at the BS. The artificial jamming can be zero-forced by the BS at each legitimate receiver via beamforming without affecting the legitimate transmission. As shown in Fig. 10, we can observe that the IRS-assisted NOMA scheme significantly outperforms the IRS-assisted OMA scheme, because the resource block (e.g., bandwidth) in NOMA can be used to serve multiple users simultaneously compared with the OMA scheme.

VI. Conclusions and Future Work

In this paper, we have proposed an IRS-assisted NOMA scheme to achieve secrecy transmission via artificial jamming, in the presence of a passive eavesdropper whose CSI is unavailable in the legitimate network. The sum rate is maximized by optimizing the transmit beamforming together with the artificial jamming vector and the IRS reflecting vector. Through the optimization, the jamming signal can be completely eliminated by SIC without affecting the legitimate transmission, and the eavesdropping can be efficiently disrupted. Due to the non-convexity, the optimization problem is first decomposed into two subproblems of the beamforming optimization and the IRS reflecting optimization. Then, each subproblem can be converted into a convex one by applying the SCA. An efficient algorithm based on alternating optimization is proposed to solve them iteratively. Simulation results are presented to show that significant secrecy performance gain can be achieved by the proposed scheme compared with the scheme without jamming and the IRS-assisted OMA scheme. In the future work, we will continue to focus on the imperfect SIC and active IRS for the proposed scheme.

References

[1] W. Wang, X. Liu, J. Tang, N. Zhao, Y. Chen, Z. Ding, and X. Wang, "Secure beamforming optimization for IRS-NOMA networks via artificial jamming," in *Proc. IEEE/CIC ICCC'21*, pp. 1–6, Xiamen, China, Jul. 2021.

[2] Q. Wu and R. Zhang, "Towards smart and reconfigurable environment: Intelligent reflecting surface aided wireless network," *IEEE Commun. Mag.*, vol. 58, no. 1, pp. 106–112, Jan. 2020.

[3] C. Huang, A. Zappone, G. C. Alexandropoulos, M. Debbah, and C. Yuen, "Reconfigurable intelligent surfaces for energy efficiency in wireless communication," *IEEE Trans. Wireless Commun.*, vol. 18, no. 8, pp. 4157–4170, Aug. 2019.

[4] H. Yu, H. D. Tuan, A. A. Nasir, T. Q. Duong, and H. V. Poor, "Joint design of reconfigurable intelligent surfaces and transmit beamforming under proper and improper gaussian signaling," *IEEE J. Sel. Areas Commun.*, vol. 38, no. 11, pp. 2589–2603, Nov. 2020.

[5] D. Xu, X. Yu, Y. Sun, D. W. K. Ng, and R. Schober, "Resource allocation for IRS-assisted full-duplex cognitive radio systems," *IEEE Trans. Commun.*, vol. 68, no. 12, pp. 7376–7394, Dec. 2020.

[6] S. Gong, X. Lu, D. T. Hoang, D. Niyato, L. Shu, D. I. Kim, and Y. C. Liang, "Toward smart wireless communications via intelligent reflecting surfaces: A contemporary survey," *IEEE Commun. Surv. Tut.*, vol. 22, no. 4, pp. 2283–2314, 4th Quart. 2020.

[7] J. Chen, Y. Liang, Y. Pei, and H. Guo, "Intelligent reflecting surface: A programmable wireless environment for physical layer security," *IEEE Access*, vol. 7, pp. 82599–82612, Jun. 2019.

[8] X. Guan, Q. Wu, and R. Zhang, "Intelligent reflecting surface assisted secrecy communication: Is artificial noise helpful or not?," *IEEE Wireless Commun. Lett.*, vol. 9, no. 6, pp. 778–782, Jun. 2020.

[9] Z. Chu, W. Hao, P. Xiao, and J. Shi, "Intelligent reflecting surface aided multi-antenna secure transmission," *IEEE Wireless Commun. Lett.*, vol. 9, no. 1, pp. 108–112, Jan. 2020.

[10] S. Hong, C. Pan, H. Ren, K. Wang, and A. Nallanathan, "Artificial-noise-aided secure MIMO wireless communications via intelligent reflecting surface," *IEEE Trans. Commun.*, vol. 68, no. 12, pp. 7851–7866, Dec. 2020.

[11] X. Yu, D. Xu, Y. Sun, D. W. K. Ng, and R. Schober, "Robust and secure wireless communications via intelligent reflecting surfaces," *IEEE J. Sel. Areas Commun.*, vol. 38, no. 11, pp. 2637–2652, Nov. 2020.

[12] Z. Ding, Y. Liu, J. Choi, Q. Sun, M. Elkashlan, I. Chih-Lin, and H. V. Poor, "Application of non-orthogonal multiple access in LTE and 5G networks," *IEEE Commun. Mag.*, vol. 55, no. 2, pp. 185–191, Feb. 2017.

[13] O. Maraqa, A. S. Rajasekaran, S. Al-Ahmadi, H. Yanikomeroglu, and S. M. Sait, "A survey of rate-optimal power domain NOMA with enabling technologies of future wireless networks," *IEEE Commun. Surv. Tut.*, vol. 22, no. 4, pp. 2192–2235, 4th Quart. 2020.

[14] A. Masaracchia, L. D. Nguyen, T. Q. Duong, C. Yin, O. A. Dobre, and E. Garcia-Palacios, "Energy-efficient and throughput fair resource allocation for TS-NOMA UAV-assisted communications," *IEEE Trans. Commun.*, vol. 68, no. 11, pp. 7156–7169, Nov. 2020.

[15] Y. Cai, Z. Qin, F. Cui, G. Y. Li, and J. A. McCann, "Modulation and multiple access for 5G networks," *IEEE Commun. Surv. Tut.*, vol. 20, no. 1, pp. 629–646, Oct. 2018.

[16] Y. Feng, S. Yan, Z. Yang, N. Yang, and J. Yuan, "Beamforming design and power allocation for secure transmission with NOMA," *IEEE Trans. Wireless Commun.*, vol. 18, no. 5, pp. 2639–2651, Mar. 2019.

[17] Y. Cao, N. Zhao, Y. Chen, M. Jin, Z. Ding, Y. Li, and F. R. Yu, "Secure transmission via beamforming optimization for NOMA networks," *IEEE Wireless Commun.*, vol. 27, no. 1, pp. 193–199, Aug. 2020.

[18] W. Wang, J. Tang, N. Zhao, X. Liu, X. Y. Zhang, Y. Chen, and Y. Qian, "Joint precoding optimization for secure swipt in UAV-aided NOMA networks," *IEEE Trans. Commun.*, vol. 68, no. 8, pp. 5028–5040, Aug. 2020.

[19] Y. Feng, S. Yan, C. Liu, Z. Yang, and N. Yang, "Two-stage relay selection for enhancing physical layer security in non-orthogonal multiple access," *IEEE Trans. Inf. Forensics Security*, vol. 14, no. 6, pp. 1670–1683, Jun. 2019.

[20] Y. Cao, N. Zhao, G. Pan, Y. Chen, L. Fan, M. Jin, and M. Alouini, "Secrecy analysis for cooperative NOMA networks with multi-antenna full-duplex relay," *IEEE Trans. Commun.*, vol. 67, no. 8, pp. 5574–5587, Apr. 2019.

[21] F. Zhou, Z. Chu, H. Sun, R. Q. Hu, and L. Hanzo, "Artificial noise aided secure cognitive beamforming for cooperative MISO-NOMA using SWIPT," *IEEE J. Sel. Areas Commun.*, vol. 36, no. 4, pp. 918–931, Apr. 2018.

[22] N. Zhao, W. Wang, J. Wang, Y. Chen, Y. Lin, Z. Ding, and N. C. Beaulieu, "Joint beamforming and jamming optimization for secure transmission in MISO-NOMA networks," *IEEE Trans. Commun.*, vol. 67, no. 3, pp. 2294–2305, Mar. 2019.

[23] X. Mu, Y. Liu, L. Guo, J. Lin, and N. Al-Dhahir, "Exploiting intelligent reflecting surfaces in NOMA networks: Joint beamforming optimization," *IEEE Trans. Wireless Commun.*, vol. 19, no. 10, pp. 6884–6898, Oct. 2020.

[24] J. Zuo, Y. Liu, Z. Qin, and N. Al-Dhahir, "Resource allocation in intelligent reflecting surface assisted NOMA systems," *IEEE Trans. Commun.*, vol. 68, no. 11, pp. 7170–7183, Nov. 2020.

[25] Z. Ding and H. Vincent Poor, "A simple design of IRS-NOMA transmission," *IEEE Commun. Lett.*, vol. 24, no. 5, pp. 1119–1123, May. 2020.

[26] J. Zuo, Y. Liu, E. Basar, and O. A. Dobre, "Intelligent reflecting surface enhanced millimeter-wave NOMA systems," *IEEE Commun. Lett.*, vol. 24, no. 11, pp. 2632–2636, Nov. 2020.

[27] C. You, B. Zheng, and R. Zhang, "Channel estimation and passive beamforming for intelligent reflecting surface: Discrete phase shift and progressive refinement," *IEEE J. Sel. Areas Commun.*, vol. 38, no. 11, pp. 2604–2620, Nov. 2020.

[28] B. Zheng, C. You, and R. Zhang, "Intelligent reflecting surface assisted multi-user OFDMA: Channel estimation and training design," *IEEE Trans. Wireless Commun.*, vol. 19, no. 12, pp. 8315–8329, Dec. 2020.

[29] M. F. Hanif, Z. Ding, T. Ratnarajah, and G. K. Karagiannidis, "A minorization-maximization method for optimizing sum rate in the downlink of non-orthogonal multiple access systems," *IEEE Trans. Signal Process.*, vol. 64, no. 1, pp. 76–88, Jan. 2016.

[30] G. Yang, X. Xu, Y. C. Liang, and M. Di Renzo, "Reconfigurable intelligent surface assisted non-orthogonal multiple access," *IEEE Trans. Wireless Commun.*, vol. 20, no. 5, pp. 3137–3151, May 2021.

[31] M. L. S. Boyd and H. Lebret, "Applications of second-order cone programming," *Lin. Alg. Applicat.*, vol. 248, pp. 193–228, Nov. 1998.

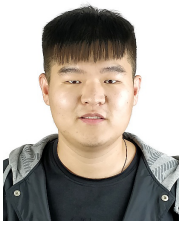

Wei Wang (Graduate Student Member, IEEE) received the B.S. degree from HeFei University of Technology, China in 2018. He is currently pursuing Ph.D. degree in the School of Information and Communication Engineering at Dalian University of Technology, China.

His current research interests include non-orthogonal multiple access, wireless power transfer and physical layer security.

Xin Liu (Senior Member, IEEE) received the M.Sc degree and the Ph.D. degree in Communication Engineering from the Harbin Institute of Technology in 2008 and 2012, respectively. He is currently an Associate Professor with the School of Information and Communication Engineering, Dalian University of Technology, China. From 2012 to 2013, he was a Research Fellow with the School of Electrical and Electronic Engineering, Nanyang Technological University, Singapore. From 2013 to 2016, he was a Lecturer with the College of Astronautics, Nanjing University of Aeronautics and Astronautics, China. His research interests include communication signal processing, cognitive radio, spectrum resource allocation and broadband satellite communications.

Jie Tang (Senior Member, IEEE) received the B.Eng. degree in Information Engineering from the South China University of Technology, Guangzhou, China, in 2008, the M.Sc. degree (with Distinction) in Communication Systems and Signal Processing from the University of Bristol, UK, in 2009, and the Ph.D. degree from Loughborough University, Leicestershire, UK, in 2012. From 2003 to 2015, he was a research associate at the School of Electrical and Electronic Engineering, University of Manchester, UK. He is currently a full professor at the School of Electronic and Information Engineering, South China University of Technology, China. His current research centers around 5G and beyond mobile communications, including topics such as massive MIMO, full-duplex communications, edge caching and fog networking, physical layer security, wireless power transfer and mobile computing. He is a senior member of IEEE, CIE and CIC, and currently serving as an Editor for IEEE Wireless Communications Letters, IEEE Access, and EURASIP Journal on Wireless Communications and Networking. He also served as a track co-chair for IEEE VTC-Spring 2018, EAI GreeNets 2019, ICCC Workshop 2019 and ICCC 2020. He is a co-recipient of the 2018 IEEE ICNC, 2018 CSPS and 2019 IEEE WCSP Best Paper Award.

Nan Zhao (Senior Member, IEEE) is currently a Professor at Dalian University of Technology, China. He received the Ph.D. degree in information and communication engineering in 2011, from Harbin Institute of Technology, Harbin, China. Dr. Zhao is serving on the editorial boards of IEEE Wireless Communications and IEEE Wireless Communications Letters. He won the best paper awards in IEEE VTC 2017 Spring, ICNC 2018, WCSP 2018 and WCSP 2019. He also received the IEEE Communications Society Asia Pacific Board Outstanding Young Researcher Award in 2018.

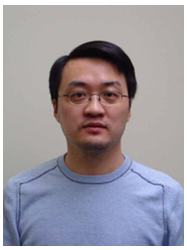

Yunfei Chen (Senior Member, IEEE) received his B.E. and M.E. degrees in electronics engineering from Shanghai Jiaotong University, Shanghai, P.R.China, in 1998 and 2001, respectively. He received his Ph.D. degree from the University of Alberta in 2006. He is currently working as an Associate Professor at the University of Warwick, U.K. His research interests include wireless communications, cognitive radios, wireless relaying and energy harvesting.

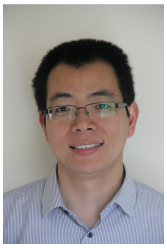

Zhiguo Ding (Fellow, IEEE) received his B.Eng in Electrical Engineering from the Beijing University of Posts and Telecommunications in 2000, and the Ph.D degree in Electrical Engineering from Imperial College London in 2005. From Jul. 2005 to Apr. 2018, he was working in Queen's University Belfast, Imperial College, Newcastle University and Lancaster University. Since Apr. 2018, he has been with the University of Manchester as a Professor in Communications. From Oct. 2012 to Sept. 2021, he has also been an academic visitor in Princeton University.

Dr Ding's research interests are 5G networks, game theory, cooperative and energy harvesting networks and statistical signal processing. He is serving as an Area Editor for the *IEEE Open Journal of the Communications Society*, an Editor for *IEEE Transactions on Vehicular Technology*, and *Journal of Wireless Communications and Mobile Computing*, and was an Editor for *IEEE Wireless Communication Letters*, *IEEE Transactions on Communications*, *IEEE Communication Letters* from 2013 to 2016. He recently received the EU Marie Curie Fellowship 2012-2014, the Top IEEE TVT Editor 2017, IEEE Heinrich Hertz Award 2018, IEEE Jack Neubauer Memorial Award 2018, IEEE Best Signal Processing Letter Award 2018, and Friedrich Wilhelm Bessel Research Award 2020. He is a Fellow of the IEEE, a Distinguished Lecturer of IEEE ComSoc, and a Web of Science Highly Cited Researcher in two categories 2020.

Xianbin Wang (Fellow, IEEE) is a Professor and Tier-1 Canada Research Chair at Western University, Canada. He received his Ph.D. degree in electrical and computer engineering from the National University of Singapore in 2001.

Prior to joining Western, he was with Communications Research Centre Canada (CRC) as a Research Scientist/Senior Research Scientist between July 2002 and Dec. 2007. From Jan. 2001 to July 2002, he was a system designer at STMicroelectronics. His current research interests include 5G/6G technologies, Internet-of-Things, communications security, machine learning and intelligent communications. Dr. Wang has over 450 highly cited journal and conference papers, in addition to 30 granted and pending patents and several standard contributions.

Dr. Wang is a Fellow of Canadian Academy of Engineering, a Fellow of Engineering Institute of Canada, a Fellow of IEEE and an IEEE Distinguished Lecturer. He has received many awards and recognitions, including Canada Research Chair, CRC President's Excellence Award, Canadian Federal Government Public Service Award, Ontario Early Researcher Award and six IEEE Best Paper Awards. He currently serves/has served as an Editor-in-Chief, Associate Editor-in-Chief, Editor/Associate Editor for over 10 journals. He was involved in many IEEE conferences including GLOBECOM, ICC, VTC, PIMRC, WCNC, CCECE and CWIT, in different roles such as general chair, symposium chair, tutorial instructor, track chair, session chair, TPC co-chair and keynote speaker. He has been nominated as an IEEE Distinguished Lecturer several times during the last ten years. Dr. Wang is currently serving as the Chair of IEEE London Section and the Chair of ComSoc Signal Processing and Computing for Communications (SPCC) Technical Committee.